The dynamics of mountain erosion: cirque growth slows as landscapes age

Iestyn D. Barr[1,2]*, Jeremy C. Ely[3], Matteo Spagnolo[4], Ian S. Evans[5], Matt D. Tomkins[6,2]

[1]Department of Natural Sciences, Manchester Metropolitan University, Manchester, M15 6BH, UK

[2]Cryosphere Research at Manchester (CRAM), Manchester, UK

[3]Department of Geography, The University of Sheffield, Sheffield, S10 2TN

[4]School of Geosciences, University of Aberdeen, Aberdeen AB24 3UF, UK

[5]Department of Geography, Durham University, Durham DH1 3LE, UK

[6]Department of Geography, School of Environment, Education and Development, University of Manchester, Manchester, M13 9PL, UK

***Correspondence**: i.barr@mmu.ac.uk

Abstract

Glacial cirques are widely used palaeoenvironmental indicators, and are key to understanding the role of glaciers in shaping mountain topography. However, notable uncertainty persists regarding the rate and timing of cirque erosion. In order to address this uncertainty, we analyse the dimensions of 2208 cirques in Britain and Ireland and model ice accumulation to investigate the degree of coupling between glacier occupation times and cirque growth. Results indicate that during the last ~120 ka, cirques were glacier-free for an average of 52.0 ± 21.2 ka (43 ± 18%); occupied by small (largely cirque-confined) glaciers for 16.2 ± 9.9 ka (14 ± 8%); and occupied by large glaciers, including ice sheets, for 51.8 ± 18.6 ka (43 ± 16%). Over the entire

Quaternary (i.e., 2.6 Ma), we estimate that cirques were glacier-free for 1.1 ± 0.5 Ma; occupied by small glaciers for 0.3 ± 0.2 Ma; and occupied by large glaciers for 1.1 ± 0.4 Ma. Comparing occupation times to cirque depths, and calculating required erosion rates reveals that continuous cirque growth during glacier occupation is unlikely. Instead, we propose that cirques attained much of their size during the first occupation of a non-glacially sculpted landscape (perhaps during the timeframe of a single glacial cycle). During subsequent glacier occupations, cirque growth may have slowed considerably, with the highest rates of subglacial erosion focused during periods of marginal (small glacier) glaciation. We propose comparatively slow rates of growth following initial cirque development because a 'least resistance' shape is formed, and as cirques deepen, sediment becomes trapped subglacially, partly protecting the bedrock from subsequent erosion. In support of the idea of rapid cirque growth, we present evidence from northern British Columbia, where cirques of comparable size to those in Britain and Ireland developed in less than 140 ka.

Keywords: Cirques, glacial erosion, erosion rate, glacial buzzsaw, Quaternary; Britain; Ireland

1. Introduction

Glacial cirques (e.g., Fig. 1) are armchair-shaped erosional hollows formed in upland environments (Evans & Cox, 1974, 1995). They are widely used as palaeoenvironmental indicators (Mîndrescu et al., 2010; Barr & Spagnolo, 2015) and are key to understanding the role of glaciers in shaping global-scale mountain topography (Oskin & Burbank, 2005; Egholm et al., 2009; Anders et al., 2010; Champagnac et al., 2012). Cirques are thought to form where glacial ice comes to

occupy, erode, and enlarge pre-existing mountainside depressions (Evans, 2006; Turnbull & Davies, 2006), eventually evolving to distinct shapes and relatively characteristic sizes (Barr & Spagnolo, 2015; Evans & Cox, 2017). However, one of the key uncertainties about cirque formation is how long they take to develop fully, with current estimates ranging from ~125 ka to a million years or more (Andrews & Dugdale, 1971; Anderson, 1978; Larsen & Mangerud, 1981; Sanders et al., 2013). Many cirques have been repeatedly occupied by glaciers during the Quaternary (Graf, 1976), but it remains unclear whether their size is the product of cumulative erosion through multiple glaciations, or is largely reached during a single glacial cycle. It is also unclear whether cirque growth continues throughout glacial occupation, even when small glaciers have evolved into valley-glaciers/ice-caps/ice-sheets, or is focused during short windows of 'active' erosion when glaciers are solely confined to their cirques (Barr & Spagnolo, 2013; Crest et al., 2017). Addressing these issues is vital if cirques are to be used as robust palaeoenvironmental indicators, and is fundamental to understanding planetary-scale landscape evolution (Banks et al., 2008; Egholm et al., 2009; Mitchell & Humphries, 2015). With this in mind, here we analyse the dimensions of cirques in Britain and Ireland, and model former ice accumulation, to permit inferences about the rate and timing of cirque growth, supported by evidence from northern British Columbia.

2. Methods

We adopt three different methods to investigate cirques in Britain and Ireland. First, we analyse cirque dimensions. Second, we model the spatial extent of the zone of ice accumulation within each cirque under different climate scenarios using a positive degree-day (temperature-index) mass balance approach. Third, we run our ice

accumulation/mass balance model throughout the timespan of a typical glacial cycle, and over the Quaternary as a whole, to estimate the duration and style of former glacier occupation within each cirque.

2.1. Analysing cirque dimensions

This work focuses on all recognisable (n = 2208) cirques in Britain and Ireland that were mapped from remotely sensed data (Barr et al., 2017; Clark et al., 2018). For each cirque, length (*L*), width (*W*), and depth (*H*) are calculated using ACME, a dedicated GIS tool (Spagnolo et al., 2017) (Fig. 1). We primarily focus on *H*, since cirque depth is largely controlled by subglacial erosion (Gordon, 1977), while controls on *L* and *W* are more complex, and likely include both glacial and periglacial processes (Sanders et al., 2012; Barr & Spagnolo, 2015).

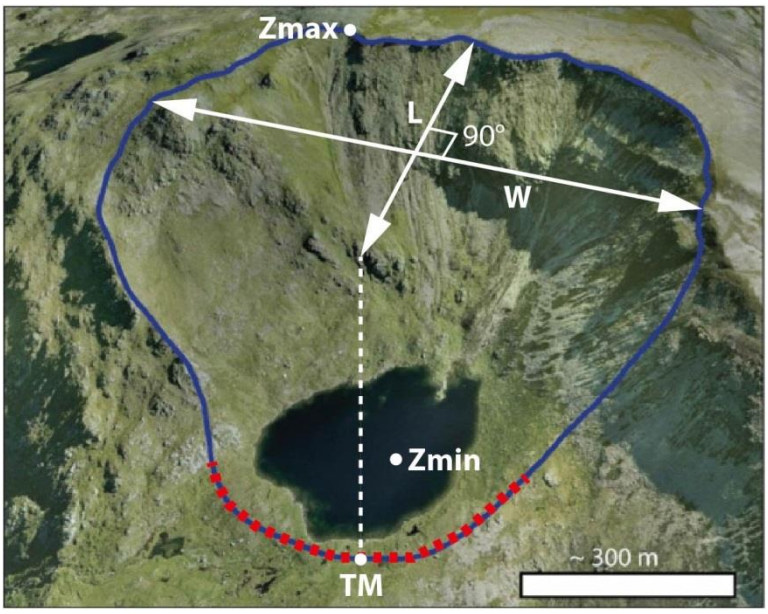

Fig. 1. Example cirque (Choire Dheirg, Scotland, 58.197°N, 4.974°W), mapped as a blue polygon. Cirque length (*L*) is the line within the cirque polygon that intersects the cirque threshold midpoint (TM—the threshold is marked as a dashed red line) and splits the polygon into two equal halves. Cirque width (*W*) is the line perpendicular to

the length and intersecting the length line midpoint. Cirque depth (*H*), not shown in the figure, is the altitudinal difference between the minimum and maximum altitude within the cirque (i.e., *Zmax* – *Zmin*). Spagnolo et al. (2017) provide further details of how these cirque metrics are calculated using their GIS tool. Background shows a getmapping ™ aerial image, viewed obliquely in Google Earth ™.

2.2. Modelling former ice accumulation

To simulate the spatial extent of the zone of former ice accumulation (*Ac*) within each cirque, we use a positive degree-day (temperature-index) mass balance model (e.g., Laumann & Reeh, 1993; Hock, 2003; Braithwaite, 2008). We do not model glacier dimensions, nor allow ice to incrementally accumulate (or ablate) year-on-year, but simply model the spatial extent of the zone of net ice accumulation within each cirque at the end of the balance year (i.e., in September) under different temperature scenarios. To achieve this, we apply equation 1 to each (30 x 30 m) pixel in a digital elevation model (DEM), and calculate *Ac* for each cirque by summing the surface area of the pixels that return positive values.

$$\sum P_m\,(snow) - \left(\sum T_m \times DDF\right) \qquad (1)$$

Where, $\Sigma\, P_m\ (snow)$ is the annual sum of mean monthly precipitation (in mm) for months with a mean near-surface temperature below a threshold value (T_{crit}). $\Sigma\, T_m$ is the annual sum of monthly positive degree-days (based on mean monthly temperatures above T_{crit}), and *DDF* is the degree-day melt factor.

In our model, T_{crit} was set at 2°C (following Harrison et al., 2014), and the *DDF* ranged from 2.6 to 4.1 mm d^{-1} $°C^{-1}$ (following Braithwaite, 2008). These values are considered representative of conditions within cirques, where melt is restricted by notable topographic shading (Hannah et al., 2000). To account for the role of solar radiation (in addition to the role of air temperature) in regulating melt, *DDFs* varied on a pixel by pixel basis, scaled according to modern annual solar radiation (calculated using the ArcGIS Solar Radiation tool). Thus, the pixel (across the entire dataset) with highest annual solar radiation was assigned a *DDF* of 4.1, and the pixel with the lowest, a value of 2.6. *DDF* was assumed to range linearly (with respect to solar radiation) between these extremes. Present-day monthly mean climatology (temperature and precipitation) was derived from gridded data (WorldClim v.2; Fick & Hijmans, 2017), which is representative of the period 1970 to 2000. Monthly climate grids were resampled from ~1 km to 30 m resolution using SRTM DEM data (vertical accuracy ~16 m). For temperature, this resampling assumed an altitudinal lapse rate of 6°C km^{-1} (Rolland, 2003), whereas precipitation was resampled (to 30 m) without applying a lapse rate. The gridded climate data (Fick & Hijmans, 2017) were selected as they incorporate observations from a dense array of weather stations, and have been widely used for environmental modelling. In each cirque, ice was allowed to accumulate on all surfaces with gradients <30° (Harrison et al., 2014). Details of model validation and sensitivity are presented in supplementary material 1.

2.3. Estimating the duration and style of glacier occupation

The purpose of modelling the spatial extent of the zone of former ice accumulation (*Ac*) within each cirque (i.e., Section 2.2.) is to estimate how long (during its history) each cirque has been glacier-free (t_{gf}); glacier-occupied (t); occupied by small (largely

cirque-confined) glaciers ($t_{marginal}$); and occupied by large glaciers (which extended beyond cirque confines) (t_{full}). Here, we assume that distinctions between these different conditions are approximated by differences in the proportion of each cirque's total surface area that is accumulating ice. Specifically, if Ac < 10% (i.e., if less than 10% of a cirque's surface area is accumulating ice), we classify cirques as glacier-free (t_{gf}), *and if* Ac ≥ 10%, we classify cirques as glacier-occupied (t). In the latter case, if Ac = 10–90%, we classify cirques as occupied by small glaciers ($t_{marginal}$); and if Ac > 90%, we classify cirques as occupied by large glaciers (t_{full}). The selection of 10% as a boundary within this scheme is justified on the assumption that when Ac < 10%, any ice within a cirque is unlikely to form a coherent and rotationally flowing glacier. The selection of 90% as a boundary is justified on the assumption that when Ac > 90%, any occupying glacier is likely to extend well beyond cirque confines. To analyse the duration and style of ice of ice occupation during the last glacial cycle (i.e., 120 ka to present), we force eq.1 with distal temperature depression (ΔT) data from the Greenland Ice Core Project (GRIP; Dansgaard et al., 1993), scaled to account for precipitation reduction with cooling climate (following Seguinot et al., 2018) for all 2208 mapped cirques (Fig. 2). To consider the duration and style of ice occupation over the Quaternary as a whole (i.e., 2.6 Ma to present), we use the composite benthic $\delta^{18}O$ stack from Lisiecki & Raymo (2005), and treat this as a proxy for temperature (thereby including the Mid-Pleistocene climate transition—Clark et al., 2006). Though there are limitations to this approach (since long-term records lack detail, and benthic $\delta^{18}O$ is not a direct proxy for terrestrial temperature), the results provide first-order estimates of Quaternary ice mass occupation times for British and Irish cirques.

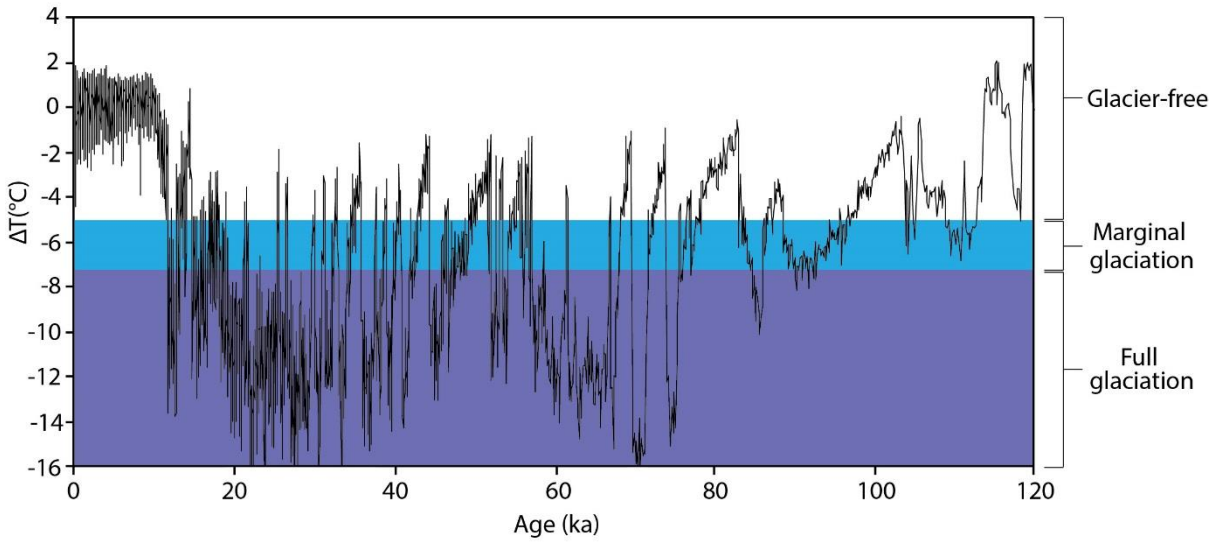

Fig. 2. Temperature offset (ΔT), relative to present, through the last glacial cycle (i.e., 120 ka to present), derived from the Greenland Ice Core Project (GRIP; Dansgaard et al., 1993), scaled to account for precipitation reduction with cooling climate (following Seguinot et al., 2018). This dataset is used to force eq. 1. Colours show periods of glacier-free conditions (white), marginal glaciation (light blue), and full glaciation (dark blue) for an example cirque (Cwm Marchlyn Mawr, Wales, 53.14°N, 4.07°W).

3. Results

3.1. Cirque dimensions

For the entire population of cirques in Britain and Ireland (Fig. 3a), *L* (mean ± 1 standard deviation = 774 ± 426 m) and *W* (786 ± 365 m) are comparable, but *H* is approximately three-times less (283 ± 108 m). All cirque size metrics have

180 approximately log-normal frequency distributions—shown for *H* in Fig. 3b.

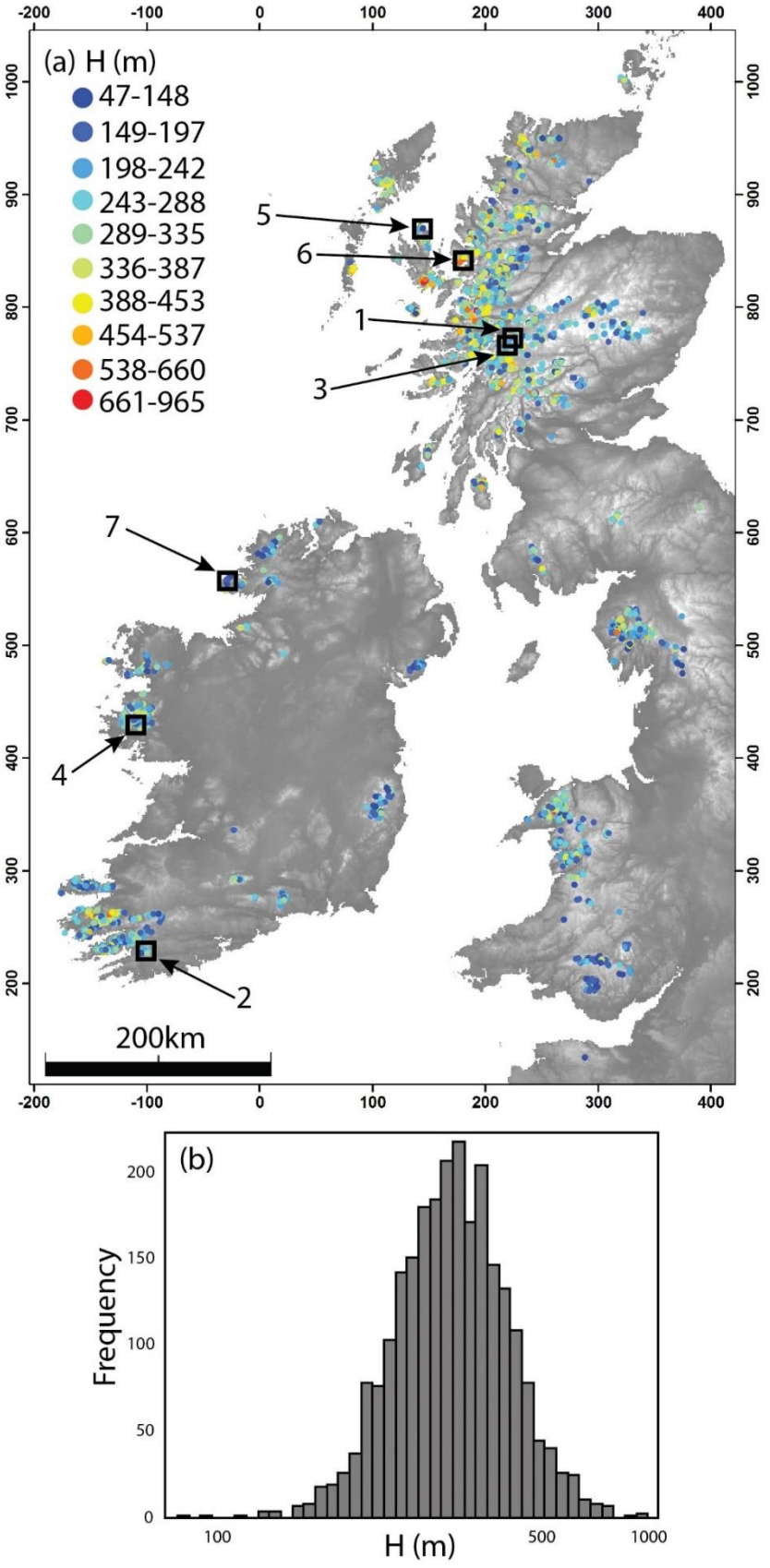

181

182

Fig. 3. Cirques in Britain and Ireland (a) coloured according to depth (*H*) (scale plotted according to the natural breaks method, which best illustrates spatial differences in these data), and (b) with *H* plotted as a frequency distribution. Note: in (b) the x-axis is plotted on a logarithmic scale. Numbers in (a) refer to cirques mentioned in the text: 1= Coire an Laoigh, 2 = Keimeen, 3 = Sron a Gharbh-Choire, 4 = Knocknahillan, 5 = Fir Bhreugach, 6 = Coire nan Arr, 7 = Lough Sallagh.

3.2. Areas of former ice accumulation

Modelling the zone of ice accumulation indicates that for individual cirques in Britain and Ireland the ΔT required for $Ac \geq 10\%$ ranges from -0.2°C (Coire an Laoigh, Scotland, 56.81°N, 4.88°W, labelled 1 in Fig, 3a) to -10.2°C (Keimeen, Ireland, 51.72°N, 9.27°W, labelled 2 in Fig, 3a), with a mean of -5.0 ± 2.1°C (i.e., ± 1σ) (Fig. 4). The ΔT required for $Ac > 90\%$ ranges from -1.6°C (Sron a Gharbh-Choire, Scotland, 56.76°N, 4.92°W, labelled 3 in Fig, 3a) to -12.3°C (Knocknahillan, Ireland, 53.52°N, 9.69°W, labelled 4 in Fig, 3a), with a mean of -6.7 ± 2.0°C (Fig. 4). The ΔT required for an individual cirque to transition from $Ac = 10\%$ to $Ac = 90\%$ ranges from -0.1°C (Fir Bhreugach, Scotland, 57.65°N, 6.28°W, labelled 5 in Fig, 3a) to -6.9°C (Coire nan Arr, Scotland, 57.42°N, 5.66°W, labelled 6 in Fig, 3a), with a mean of -1.7 ± 0.9°C (Fig. 4).

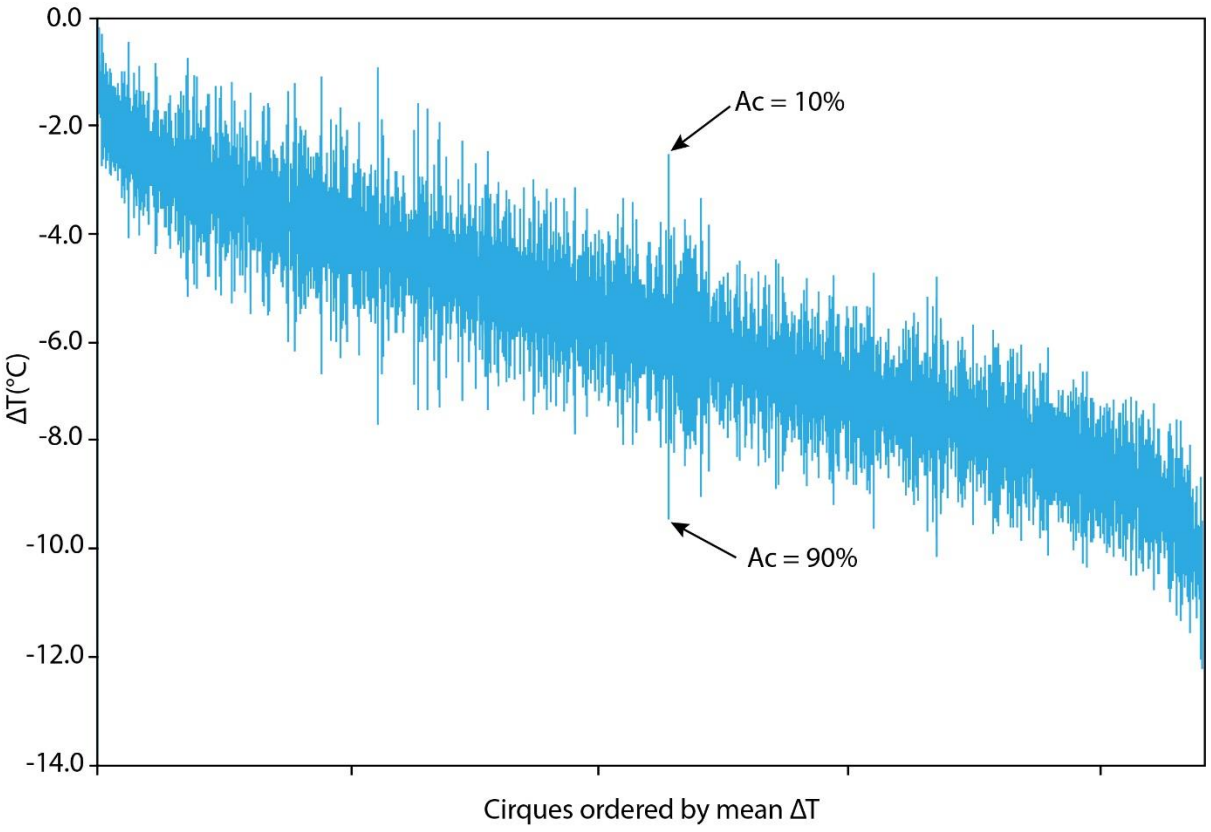

Fig. 4. Modelled temperature offset (ΔT°C), relative to present, required to accumulate ice within the cirques of Britain and Ireland. This figure shows the ΔT required for between 10% and 90% of each cirque's surface area to be accumulating ice. The example indicated by arrows is Coire nan Arr, Scotland (57.42°N, 5.66°W; labelled 6 in Fig, 3a), which is the cirque that requires the greatest ΔT (i.e., -6.9°C) to transition from *Ac* = 10% to *Ac* = 90%.

3.3. Duration and style of glacier occupation

Using ice accumulation modelling and published ΔT data, we estimate that during the last glacial cycle, cirques in Britain and Ireland were glacier-free (t_{gf}) for between 11.5 ka (Coire an Laoigh), and 93.6 ka (Keimeen), with a mean of 52.0 ± 21.2ka (43 ± 18%) (Fig. 5), and glacier-occupied (t) for between 26.4 ka and 108.5 ka, with a mean of 68.0 ± 21.2 ka (57 ± 18%). When occupied, cirques contained small (largely cirque-confined) glaciers ($t_{marginal}$) for between 0.9 ka (Lough Sallagh, Ireland, 54.74°N,

8.67°W, labelled 7 in Fig, 3a) and 64.2 ka (Coire nan Arr, Scotland), with a mean of 16.2 ± 9.9 ka (14 ± 8%) (Fig. 5); and large glaciers (which extended beyond cirque confines), including ice sheets, (t_{full}) for between 12.7 ka (Knocknahillan, Ireland, 53.51°N, 9.70°W) and 101.0 ka (Sron a Gharbh-Choire, Scotland, 56.76°N, 4.92°W), with a mean of 51.8 ± 18.6 ka (43 ± 16%) (Fig. 5). To investigate possible relationships between the duration and style of glacier occupation and resulting cirque depth, *H* is compared to t_{gf}, t, $t_{marginal}$, and t_{full} (Fig. 6). These plots show a weak, but statistically significant ($p < 0.01$), positive relationship between t and H ($r^2 = 0.11$; Fig. 6a), and a statistically significant positive relationship between $t_{marginal}$ and H ($r^2 = 0.49$; Fig. 6b). However, in the latter case, caution should be applied when interpreting this relationship since it partly reflects the control that H exerts on $t_{marginal}$ (i.e., due to altitudinal controls on temperature, deep cirques take comparatively long to transition from Ac = 10% to Ac = 90%), rather than vice-versa. The control that H exerts on $t_{marginal}$ is demonstrated by the statistically significant relationship between H and the ΔT required for individual cirques to transition from Ac = 10% to Ac = 90% ($r^2 = 0.51$; Fig. 6d). There is no relationship between H and t_{full} ($r^2 = 0.00$; Fig. 6c).

There are clear regional patterns in t and t_{full} (Fig. 7), with cirques in Scotland, for example, having experienced ice occupation for most (> 100 ka) of the last glacial cycle, and those in SW Ireland and south Wales having experienced occupation for a far shorter period (< 40 ka) (Fig. 7a). Notably, H does not show a correspondingly clear spatial pattern across Britain and Ireland (Fig. 3a).

When considering the Quaternary as a whole (based on Lisiecki & Raymo, 2005), we estimate that cirques in Britain and Ireland were glacier-free (t_{gf}) for 1.1 ± 0.5 Ma, and glacier-occupied (t) for 1.5 ± 0.5 Ma. When occupied, cirques contained small (largely cirque-confined) glaciers ($t_{marginal}$) for 0.3 ± 0.2 Ma; and large glaciers,

including ice sheets, (t_{full}) for 1.1 ± 0.4 Ma. Given the long time period considered, these estimates are less precise than those based on the last glacial cycle alone.

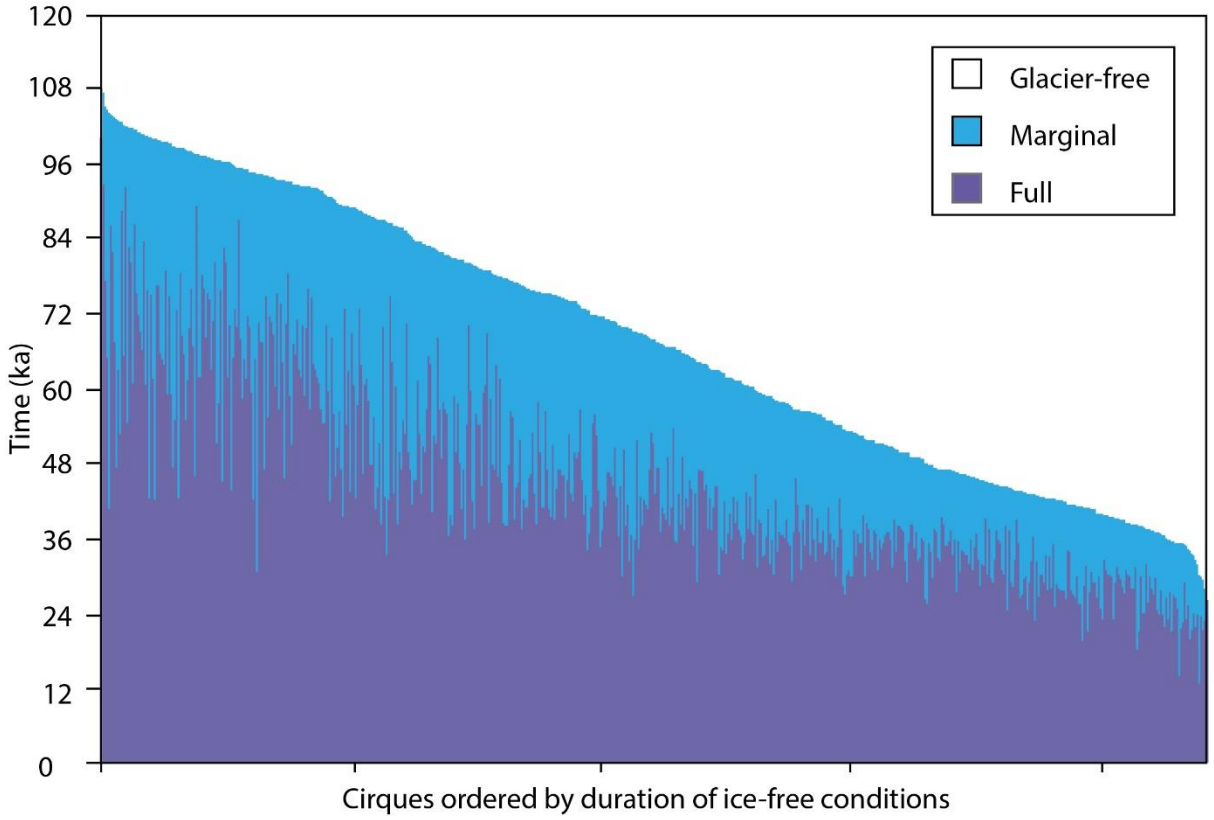

Fig. 5. Cirques in Britain and Ireland, classified according to the duration of the last glacial cycle (120 ka to present) that our modelling suggests they were glacier-free (i.e., t_{gf} ; *Ac* < 10%); occupied by small (marginal), largely cirque-confined, glaciers (i.e., $t_{marginal}$; *Ac* 10–90%); and occupied by large glaciers (which extended beyond cirque confines) (i.e., t_{full}; *Ac* > 90%).

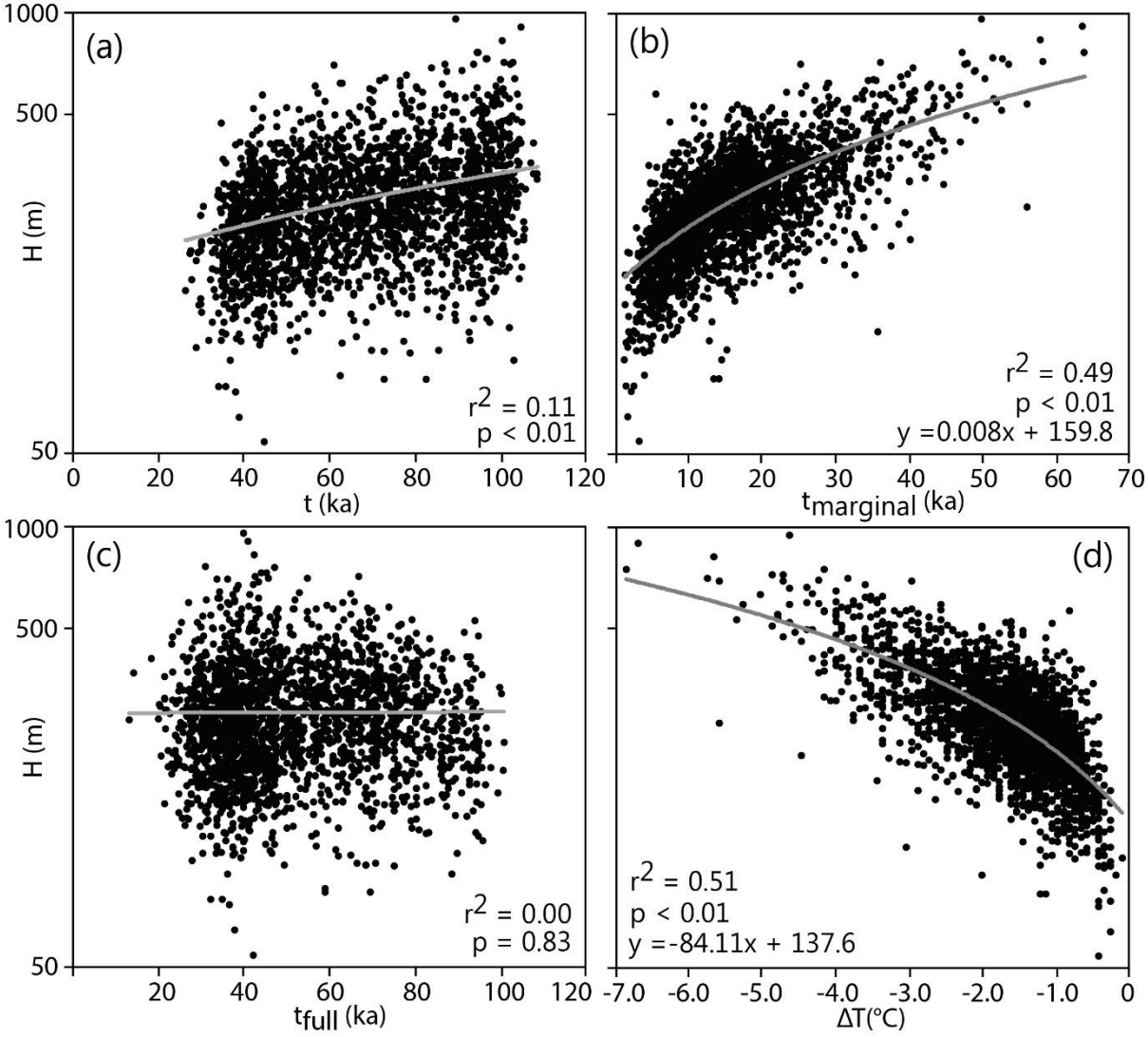

Fig. 6. Cirque depth (*H*) in Britain and Ireland plotted against the duration of the last glacial cycle (120 ka to present) that our modelling suggests they were (a) glacier-occupied (*t*); (b) occupied by small (largely cirque-confined) glaciers ($t_{marginal}$); and (c) occupied by large glaciers (which extended beyond cirque confines) (t_{full}). (d) *H* plotted against the ΔT required for individual cirques to transition from *Ac* = 10% to *Ac* = 90% Note: in all examples, the y-axes are plotted on logarithmic scales.

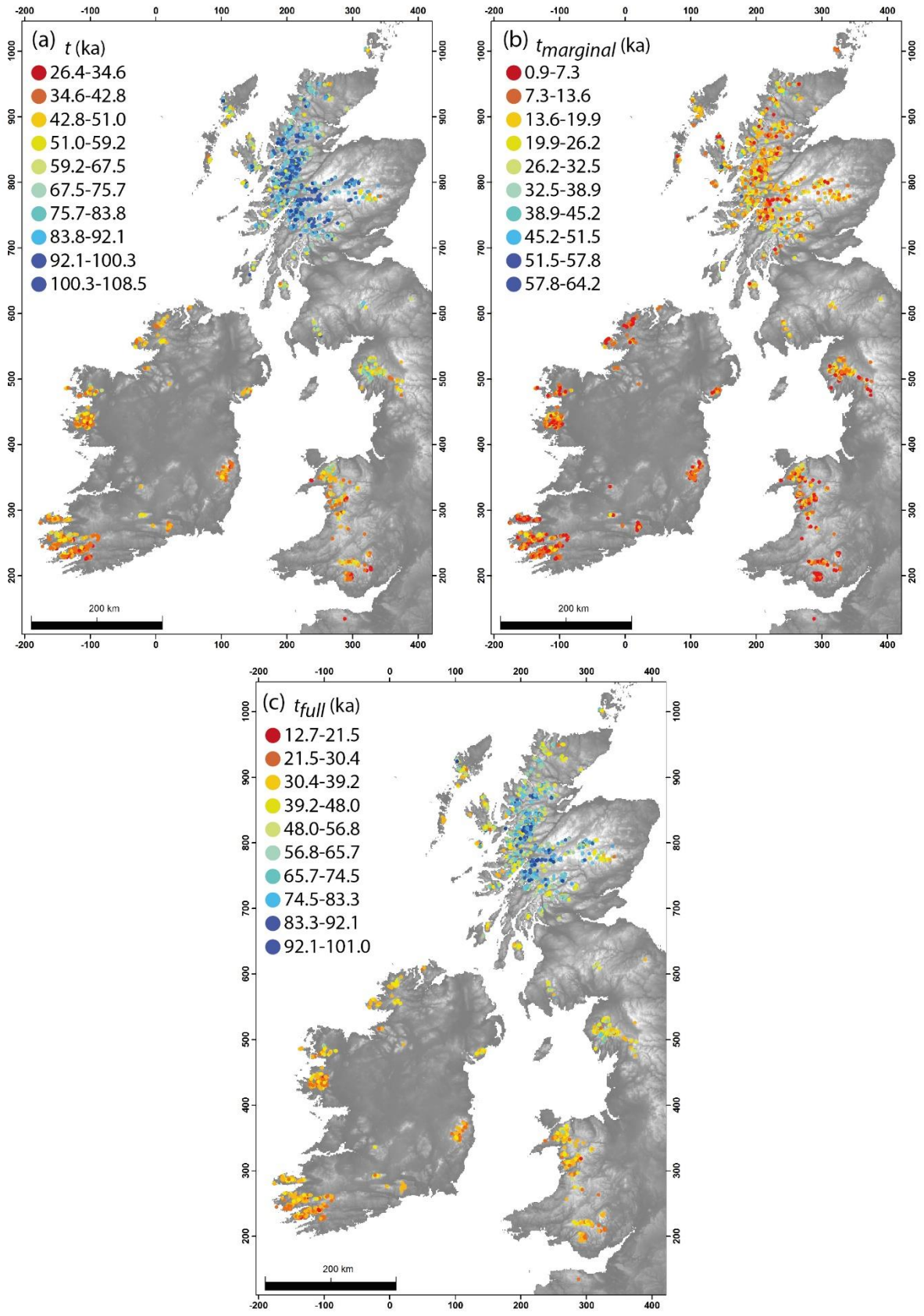

262

263 Fig. 7. Spatial variability in the duration of the last glacial cycle (120 ka to present) that

264 our modelling suggests cirques in Britain and Ireland were (a) glacier-occupied (*t*); (b)

occupied by small (largely cirque-confined) glaciers ($t_{marginal}$); and (c) occupied by large glaciers (which extended beyond cirque confines) (t_{full}).

4. Discussion

4.1. Evidence against continuous cirque growth

Ice accumulation modelling suggests that during the last glacial cycle, cirques in Britain and Ireland experienced glacier/ice-sheet occupation (*t*) for an average of 68.0 ± 21.2 ka. Over the Quaternary as a whole (based on Lisiecki & Raymo, 2005), modelling suggests 1.5 ± 0.5 million years of glacier/ice occupation. Given a mean cirque depth of 283 ± 108 m, and assuming a fluvial valley-head with an initial depth of 50–100 m (Lewis. 1949), continuous cirque growth throughout this period of occupation would imply an average vertical erosion rate of ~0.14 mm a^{-1}. Such an erosion rate is possible, but lies towards the low end of published estimates, and modern cirque glaciers suggest that vertical erosion rates can be an order of magnitude higher (Table 1). In addition, since our estimate of cirque erosion is based on *H*—i.e., the altitudinal difference between the minimum and maximum altitude of a cirque (Fig. 1)—it likely represents the maximum erosion rate per cirque, since other parts of the cirque have lower maximum and/or higher minimum elevations, and therefore require the excavation of less bedrock. Importantly, if cirque growth is continuous during ice occupation, then cirque depth would be expected to scale linearly with *t* and match clear spatial patterns in *t*. However, the relationship between *H* and *t* is weak (Fig. 6a) and the match in spatial patterns is not present (Fig. 7a vs. Fig. 3a). Thus, our results indicate that constant and continuous vertical erosion of cirques throughout glacier occupation is an unlikely scenario.

290

291 Table 1. A global dataset of published cirque erosion rates, modified from Barr &

292 Spagnolo (2015).

Location	Vertical erosion (mm a^{-1})	Headward erosion (mm a^{-1})	Sidewall erosion (mm a^{-1})	Citation
Marie Byrd Land, Antarctica	0.4	5.8	0.8	Andrews & LeMasurier (1973)
Arapaho Glacier, Front Range, Colorado, USA	0.095–0.17	-	-	Reheis (1975)
Pangnirtung Fiord, Baffin Island, Canada	0.008–0.076	-	-	Anderson (1978)
Kråkenes, Norway	0.5–0.6	0.1	-	Larsen & Mangerud (1981)
Rocky Mountains	0.147–1.811	-	-	Olyphant (1981)
Ivory Lake, Southern Alps, New Zealand	5.3–5.9	-	-	Hicks et al. (1990)
Ovre Beiarbreen, Norway	0.18	-	-	Bogen (1996)

Ben Ohau Range, New Zealand	0.29	0.44	-	Brook et al. (2006)
Nisqually Glacier, Washington, USA	5.0	-	-	Mills (1979)
Canadian Rocky Mountains, British Columbia	0.5–0.9	1.2	-	Sanders et al. (2013)

293

294 **4.2. Evidence for episodic cirque growth**

295 There is evidence from published literature (Barr & Spagnolo, 2013; Crest et al., 2017)
296 to suggest that during glacier occupation, the rate of cirque growth fluctuates
297 considerably. This suggest that cirque erosion predominantly occurs during periods of
298 marginal glaciation, and may reduce (or even stop) when the landscape is occupied
299 by larger ice masses (Barr & Spagnolo, 2013; Crest et al., 2017). The logic behind this
300 assumption is that when glaciers are small, subglacial erosion is focused at the cirque
301 floor and base of the cirque headwall (Barr & Spagnolo, 2015). By contrast, larger
302 glaciers and ice sheets extend well beyond cirque confines, and focus erosion further
303 down-valley (Derbyshire & Evans, 1976). Under such conditions, cirques themselves
304 may become occupied by cold-based, low-gradient, and therefore minimally erosive
305 glacial ice (Cook & Swift, 2012; Barr & Spagnolo, 2013, 2015; Crest et al., 2017), as
306 the glacier surface slope becomes decoupled from bed slope, and basal sheer
307 stresses are reduced (Pedersen et al., 2014). At present, the only observational
308 evidence to support this idea comes from the east-central Pyrenees, where Crest et
309 al. (2017) found erosion rates during periods of cirque-type glaciation to be notably
310 greater than when cirques were occupied by an extensive icefield (i.e., 0.03–0.35 mm

311 a^{-1} vs. 0–0.03 mm a^{-1})—though still generally low when compared to values in Table
312 1. In Britain and Ireland, ice accumulation modelling suggests that during the last
313 glacial cycle, cirques experienced marginal glacial conditions for an average of 16.2 ±
314 9.9 ka, and full (extensive) glacial conditions for 51.8 ± 18.6 ka. If erosion rates from
315 the east-central Pyrenees (Crest et al., 2017) are applied to Britain and Ireland, and
316 we focus on cirque deepening alone, this implies that during the last glacial cycle,
317 cirque depth increased by 3.1 ± 1.9 m during periods of marginal glaciation, and only
318 0.8 ± 0.3 m during full glacial conditions. The minimal impact of full glacial conditions
319 might explain the clear lack of relationship between t_{full} and cirque size (Fig. 6c). Over
320 the Quaternary as a whole, this approach implies a cumulative 66 ± 40 m of cirque
321 deepening during periods of marginal glaciation, and 23 ± 8 m of deepening during full
322 glacial conditions. Assuming a fluvial valley-head with an initial depth of 50–100 m
323 (Lewis, 1949), these estimates of cumulative Quaternary erosion result in cirque
324 depths lower than the mean cirque depth of 283 ± 108 m observed in Britain and
325 Ireland. This might indicate that overall cirque erosion rates in Britain and Ireland were
326 higher than in the Pyrenees, though cirque depths in these regions are typically
327 comparable (Delmas et al., 2014). An alternative explanation is that erosion rates from
328 'recent' glaciations are not representative of earlier periods, and that cirque growth
329 slows as they age. Thus, using erosion rates from 'recent' glaciations to extrapolate
330 throughout the Quaternary is likely to underestimate total cirque erosion.
331
332 **4.3. A conceptual model for cirque growth**
333 Evidence from the present study supports the idea that cirque growth is
334 episodic, focused during periods of marginal glaciation and slowing considerably
335 during full glacial conditions. However, we also propose that when cirques first

initiate—i.e., when sizable glaciers first come to occupy a non-glacially sculpted landscape—erosion rates are likely to be particularly rapid, allowing cirques to attain much of their size very quickly. Our suggestion is that as cirques rapidly grow from pre-existing topographic depressions (driven by high erosion rates), they start to attain 'least-resistance' shapes (i.e., armchair-shaped hollows), which allow ice to be efficiently evacuated with minimal erosional impact. In attaining 'least-resistance' shapes, cirques often become overdeepened, thereby trapping subglacial sediment at their floors (Cook & Swift, 2012). This sediment may further reduce cirque erosion (deepening) by acting as a protective layer between the ice and bedrock at the cirque floor (Hooke, 1991; Gądek et al., 2015). In this scenario, spatial differences in the duration of glacier occupation become less important in regulating cirque size. This might explain why there is limited spatial pattern in cirque depth across Britain and Ireland (Fig. 3a), despite clear, and order of magnitude, differences in t (Fig. 7a). However, cirque depth does vary locally, and this variability might reflect differences in $t_{marginal}$; differences in glacier dynamics during periods of marginal glaciation; differences in the efficiency of sediment evacuation; and/or other factors such as bedrock structure and lithology (Barr & Spagnolo, 2015).

Evidence to support the notion that cirques grow rapidly (as suggested above) is rare, often because the timing of cirque initiation is extremely difficult to constrain (Turnbull & Davies, 2006; Barr & Spagnolo, 2015). Developments in surface exposure dating potentially allow the timing of cirque de-activation (i.e., deglaciation) to be determined (Barth et al., 2016, 2018). However, there are very few locations where the timing of cirque initiation can be constrained with any certainty. One circumstance where chronologies of cirque initiation can be constrained is where cirques are eroded into tuyas (flat-topped volcanoes formed subglacially), which often have a clear and

chronologically constrainable history. A classic example is Tuya Butte, northern British Columbia, which formed c.140 ka (Smellie & Edwards, 2016). Two glacial cirques are present at its northern end (Mathews, 1947; Allen et al., 1982) (Fig. 8) which, given the tuya's history, must have formed within the past 140 ka (i.e., during a single glacial cycle). These cirques have depths of 185 and 210 m. The lithology of this area is not directly comparable to that of the cirques of Britain and Ireland, which comprise 34 distinct geological units, ranging in strength from granites to mudstones (Barr et al., 2017). However, it is not obviously much weaker, as Tuya Butte is composed of weak palagonitized hyaloclastite agglomerate capped by ~80 m of thick, massive lava flow basalt, likely comparatively resistant to glacial erosion (Allen et al., 1982; Smellie, 2017). If cirques in Britain and Ireland attained similar dimensions to those at Tuya Butte during a single glacial cycle (from an initial depression depth of 50–100 m), this would suggest erosion rates (during this period) of 1.0–3.4 mm a^{-1}, if continuous during ice occupation; and 3.3–25.4 mm a^{-1}, if confined to periods of marginal glaciation. Attaining such sizes during a single glacial cycle would also imply that cirque erosion rates were an order of magnitude lower over the rest of the Quaternary – i.e., 0.05–0.16 mm a^{-1}, if continuous during ice occupation; and 0.16–1.24 mm a^{-1}, if confined to periods of marginal glaciation. Note, it is worth emphasising that, since these erosion rates are based on *H*, they likely represent the maximum values per cirque (see Section 4.1.).

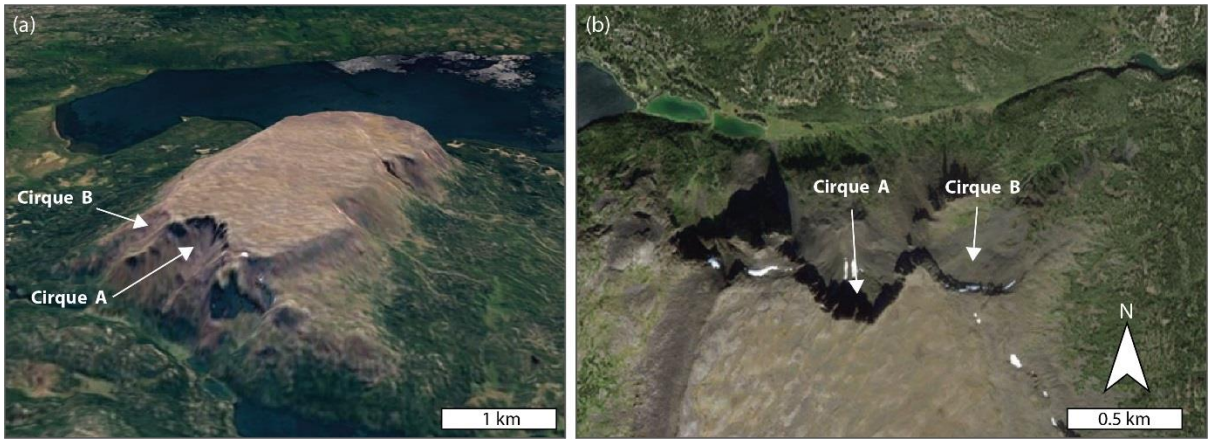

Fig. 8. Tuya Butte, northern British Columbia. (a) Landsat image viewed obliquely (from the northwest) in Google Earth™. (b) PlanetScope satellite image, clearly showing the two cirques (A = 59.136°N, 130.570°W; B = 59.137°N, 130.560°W) eroded into the tuya's northern flank.

4.4. Implications for understanding cirque erosion rates

The conceptual model we propose here is that cirques grow quickly when they first initiate – perhaps attaining much of their size, and reaching a least-resistance shape, during a single glacial cycle. Thereafter (i.e., during subsequent phases of glaciation), cirque growth slows by an order of magnitude, and is perhaps focused during periods of marginal glaciation. This model is partly supported by broader scale glacial erosion rate data (i.e., not derived from cirques explicitly) (Hallet et al., 1996; Koppes & Montgomery, 2009), and modelling of glacial erosion over multiple glacial-interglacial cycles (MacGregor et al., 2009; Egholm et al., 2012). For example, Koppes & Montgomery (2009) note that both fluvial and glacial erosion rates are typically highest for landscapes forced out of equilibrium (e.g., following volcanic eruptions, or during glacial retreat). We suggest that the first glacial occupation of a non-glacially sculpted landscape is an extreme example of a shift in equilibrium state – explaining high erosion rates during such periods. Koppes & Montgomery (2009) report that modern

temperate tidewater glaciers (i.e., retreating glaciers, not in climatic equilibrium) typically have erosion rates in the 10–100 mm a^{-1} range. In Britain and Ireland, we suggest that erosion rates of comparable magnitude (i.e., 3.3–25.4 mm a^{-1}) would be required to allow cirques the size of those at Tuya Butte to form during a single glacial cycle (if erosion was confined to periods of marginal glaciation)—such rates are up to an order of magnitude higher than observed for modern cirque glaciers (Table 1). Over the rest of the Quaternary, we suggest erosion rates (i.e., 0.16–1.24 mm a^{-1}) that are generally comparable with estimates from the Pyrenees (Crest et al., 2017) and derived from modern cirque glaciers globally (Table 1), with some exceptions which are notably higher (i.e., up to 6.0 mm a^{-1}; Table 1). However, these exceptionally high published erosion rate estimates are often based on sediment volumes within proglacial streams/forelands (Reheis, 1975; Anderson, 1978; Larsen & Mangerud, 1981; Hicks et al., 1990; Bogen, 1996; Sanders et al., 2013), and some of this sediment may have been stored under glaciers for a considerable period (as noted by Koppes & Montgomery, 2009). It is therefore possible that such estimates are a measure of the rate at which sediment is being evacuated from the cirque, rather than the rate at which bedrock is being eroded.

In all, we suggest that erosion rate estimates derived from modern cirque glaciers are representative of periods of marginal glaciation, rather than longer-term averages; and may be biased by temporal decoupling of bedrock erosion and sediment evacuation.

4.5. Implications for understanding landscape evolution

The discussion above supports the idea that cirque erosion largely occurs during comparatively short periods of marginal (small-scale) glacier occupation, and that

426 cirques attain much of their size during the first occupation of a non-glacially sculpted
427 landscape (particularly susceptible to erosion). This raises questions about the role of
428 glaciers in long-term landscape evolution, particularly in relation to the buzzsaw
429 hypothesis, which suggests that glacial erosion can keep pace with rates of tectonic
430 uplift, and act as a fundamental limit to mountain height at a near-global scale
431 (Brozović et al., 1997; Egholm et al., 2009; Pedersen et al., 2010; Mitchell &
432 Humphries, 2015). The suggestion that cirque erosion is largely focused during an
433 early phase of glaciation is difficult to reconcile with the buzzsaw hypothesis: however,
434 the suggestion that subsequent erosion may be episodic, is not. For example, during
435 periods of marginal glaciation, rates of erosion may (in some cases) be comparable to
436 uplift rates (e,g, Crest et al., 2017). By contrast, during full glacial conditions, rates of
437 erosion are likely to be significantly lower but, during such periods, tectonic uplift is
438 also likely to be reduced due to glacio-isostatic depression. Thus, a cycle might
439 develop, whereby low erosion rates are tied to periods of low uplift, and vice versa,
440 allowing the glacial buzzsaw to operate, limiting mountain height, throughout cycles of
441 Quaternary glaciation.
442
443 **4.6. Implications for interpreting cirque depth**
444 Spatial variability in cirque depth (within and between regions) has been used
445 previously to infer palaeoenvironmental conditions, on the assumption that cirque size
446 is largely dictated by the duration of glacier occupation, and by ice dynamics (i.e., the
447 intensity of erosion) during such periods (e.g., Barr & Spagnolo, 2015). However,
448 results from the present study suggest that cirque size is largely determined during an
449 early stage of glaciation, and (to a lesser degree) during short phases of subsequent
450 active erosion when glaciers are small. Given the suggestion that growth continues,

but slowly, following an initial phase of glaciation, it is likely that the ergodic principle, whereby variation in feature size can be substituted (to some degree) for variation with time, can still be applied to cirques (Olyphant, 1981; Evans, 2006). However, spatial differences in cirque depth will reflect differences in bedrock lithology and structure (Barr & Spagnolo, 2015), as well as differences in conditions (e.g. differences in glacier dynamics) during the initial phase of glaciation, and perhaps during short (active) periods during subsequent glacier occupation. Thus, spatial differences in cirque depth may reflect the complex interplay of controls, leading to difficulties with using cirque depth as robust source of palaeoenvironmental information.

5. Conclusions

In this study, we analyse the size characteristics of cirques in Britain and Ireland, to reveal information about the rate and timing of their growth. Ice accumulation modelling indicates that the temperature depression, relative to present, required for ≥ 10% of a cirque's surface area to be accumulating ice ranges from -0.2°C to -10.2°C, with a mean of -5.0 ± 2.1°C. These temperature depression data suggest that during the last glacial cycle (i.e., 120 ka to present), cirques in Britain and Ireland were glacier-free for an average of 52.0 ± 21.2 ka; occupied by small (largely cirque-confined) glaciers for 16.2 ± 9.9 ka; and occupied by large glaciers for 51.8 ± 18.6 ka. Over the Quaternary as a whole, modelling indicates that cirques were glacier-free for 1.1 ± 0.5 Ma; occupied by small glaciers for 0.3 ± 0.2 Ma; and occupied by large glaciers for 1.1 ± 0.4 Ma. We suggest that continuous cirque growth during periods of glacier occupation is unlikely since spatial patterns in cirque size fail to match patterns in glacier-occupation time. A more realistic proposition is that during glacier occupation, cirque growth is episodic, and is maximised during periods of marginal

glaciation, and may greatly reduce, or even stop, when the landscape is occupied by larger ice masses. We propose a conceptual model for cirque growth, whereby cirques attain much of their size when they first initiate (i.e., when glaciers first come to occupy a non-glacially sculpted landscape). This might occur during a single glacial cycle. Following this period (and despite potentially repeated glacier occupation), cirque growth slows by an order of magnitude, and, even then, is largely focused during periods of marginal glaciation. We propose generally slow rates of growth following initial cirque development because a least resistance shape is likely to form and, as cirques deepen, sediment becomes trapped subglacially, partly protecting the bedrock from subsequent erosion. In support of the idea that much of a cirque's growth can occur during a single glacial cycle, we present evidence from northern British Columbia, where cirques are eroded into Tuya Butte – a flat-topped, formerly subglacial, volcano formed c.140 ka. Based on this evidence, we suggest that erosion rates derived from modern cirque glaciers are unlikely to be representative of longer-term conditions and primarily measure the rate at which sediment is being evacuated from cirques, which relates only indirectly to the rate at which bedrock is being eroded. Finally, our modelling suggests that palaeoenvironmental inferences made from cirque depth should be treated with caution, as cirque characteristics are primarily controlled by the initial phase of glaciation, and are perhaps modified during short periods of marginal glaciation.

Acknowledgments

JCE acknowledges a NERC independent research fellowship grant number NE/R014574/1. We also thank the associate editor and two anonymous reviewers for their corrections, comments and suggestions.

References

Allen, C. C., Jercinovic, M. J. & Allen, J. S. (1982). Subglacial volcanism in north-central British Columbia and Iceland. *The Journal of Geology*, 90(6), 699–715. Doi: 10.1086/628725

Andrews, J. T., & Dugdale, R. E. (1971). Late Quaternary glacial and climatic history of northern Cumberland Peninsula, Baffin Island, NWT, Canada. Part V: Factors affecting corrie glacierization in Okoa Bay. *Quaternary Research*, 1, 532–551. Doi: 10.1016/0033-5894(71)90063-9

Andrews, J. T., & LeMasurier, W. E. (1973). Rates of Quaternary glacial erosion and corrie formation, Marie Byrd Land, Antarctica. *Geology*, 1(2), 75–80. Doi: 10.1130/0091-7613(1973)1<75:ROQGEA>2.0.CO;2

Anders, A. M., Mitchell, S. G., & Tomkin, J. H. (2010). Cirques, peaks, and precipitation patterns in the Swiss Alps: Connections among climate, glacial erosion, and topography. Geology, 38 (3). 239–242. Doi: 10.1130/G30691.1

Anderson, L. W. (1978). Cirque glacier erosion rates and characteristics of Neoglacial tills, Pangnirtung Fiord area, Baffin Island, NWT, Canada. *Arctic and Alpine Research*, 10 (4), 749–760. Doi: 10.1080/00040851.1978.12004012

Banks, M. E., McEwen, A. S., Kargel, J. S., Baker, V. R., Strom, R. G., Mellon, M. T., … Jaeger, W.L. (2008). High Resolution Imaging Science Experiment (HiRISE) observations of glacial and periglacial morphologies in the circum-Argyre Planitia highlands, Mars. *Journal of Geophysical Research: Planets*, 113(E12). Doi: 10.1029/2007JE002994

524 Barr, I. D., & Spagnolo, M. (2013). Palaeoglacial and palaeoclimatic conditions in the NW
525 Pacific, as revealed by a morphometric analysis of cirques upon the Kamchatka
526 Peninsula. *Geomorphology*, 192, 15–29. Doi: 10.1016/j.geomorph.2013.03.011
527 Barr, I. D., & Spagnolo, M. (2015). Glacial cirques as palaeoenvironmental indicators:
528 Their potential and limitations. *Earth-science reviews*, 151, 48–78. Doi:
529 10.1016/j.earscirev.2015.10.004
530 Barr, I. D., Ely, J. C., Spagnolo, M., Clark, C. D., Evans, I. S., Pellicer, X. M., … Rea, B.
531 R. (2017). Climate patterns during former periods of mountain glaciation in Britain
532 and Ireland: Inferences from the cirque record. *Palaeogeography,*
533 *Palaeoclimatology, Palaeoecology*, 485, 466–475. Doi:
534 10.1016/j.palaeo.2017.07.001
535 Barth, A. M., Clark, P. U., Clark, J., McCabe, A. M. & Caffee, M. (2016). Last Glacial
536 Maximum cirque glaciation in Ireland and implications for reconstructions of the
537 Irish Ice Sheet. *Quaternary Science Reviews*, 141, 85–93. Doi:
538 10.1016/j.quascirev.2016.04.006
539 Barth, A. M., Clark, P. U., Clark, J., Roe, G. H., Marcott, S. A., McCabe, A. M., … Dunlop,
540 P. (2017). Persistent millennial-scale glacier fluctuations in Ireland between 24 ka
541 and 10 ka. *Geology*, 46(2), 151–154. Doi: 10.1130/G39796.1
542 Bogen, J. (1996). Erosion rates and sediment yields of glaciers. *Annals of Glaciology*, 22,
543 48–52. Doi: 10.3189/1996AoG22-1-48-52
544 Braithwaite, R. J. (2008). Temperature and precipitation climate at the equilibrium-line
545 altitude of glaciers expressed by the degree-day factor for melting snow. *Journal*
546 *of Glaciology*, 54(186), 437–444. Doi: 10.3189/002214308785836968
547 Brook, M. S., Kirkbride, M. P., & Brock, B. W. (2006). Cirque development in a steadily
548 uplifting range: rates of erosion and long-term morphometric change in alpine

549 cirques in the Ben Ohau Range, New Zealand. *Earth Surface Processes and*
550 *Landforms*, 31(9), 1167–1175. Doi: 10.1002/esp.1327
551 Brozović, N., Burbank, D. W., & Meigs, A. J. (1997). Climatic limits on landscape
552 development in the northwestern Himalaya. *Science*, 276(5312), 571–574. Doi:
553 10.1126/science.276.5312.571
554 Champagnac, J. D., Molnar, P., Sue, C. & Herman, F. (2012). Tectonics, climate, and
555 mountain topography. *Journal of Geophysical Research: Solid Earth*, 117(B2).
556 Doi: 10.1029/2011JB008348
557 Clark, C. D., Ely, J. C., Greenwood, S. L., Hughes, A. L., Meehan, R., Barr, I. D., …
558 Jordan, C. J. (2018). BRITICE Glacial Map, version 2: a map and GIS database
559 of glacial landforms of the last British–Irish Ice Sheet. *Boreas*, 47(1), 11–27. Doi:
560 10.1111/bor.12273
561 Clark, P. U., Archer, D., Pollard, D., Blum, J. D., Rial, J. A., Brovkin, V., Mix, A. C., Pisias,
562 N. G. & Roy, M. (2006). The middle Pleistocene transition: characteristics,
563 mechanisms, and implications for long-term changes in atmospheric
564 pCO_2. *Quaternary Science Reviews*, *25*(23-24), 3150–3184. Doi:
565 10.1016/j.quascirev.2006.07.008
566 Cook, S. J., & Swift, D. A. (2012). Subglacial basins: their origin and importance in glacial
567 systems and landscapes. *Earth-Science Reviews*, 115(4), 332–372. Doi:
568 10.1016/j.earscirev.2012.09.009
569 Crest, Y., Delmas, M., Braucher, R., Gunnell, Y., Calvet, M., & ASTER Team. (2017).
570 Cirques have growth spurts during deglacial and interglacial periods: Evidence
571 from ^{10}Be and ^{26}Al nuclide inventories in the central and eastern
572 Pyrenees. *Geomorphology*, 278, 60–77. Doi: 10.1016/j.geomorph.2016.10.035

573 Dansgaard, W., Johnsen, S. J., Clausen, H. B., Dahl-Jensen, D., Gundestrup, N. S.,
574 Hammer, C. U., … Bond, G. (1993). Evidence for general instability of past climate
575 from a 250-kyr ice-core record. *Nature*, 364(6434), 218–220. Doi:
576 10.1038/364218a0
577 Derbyshire, E., & Evans, I.S. (1976). The climatic factor in cirque variation. In Derbyshire,
578 E. (Ed.), *Geomorphology and Climate* (pp. 447–494). Chichester: John Wiley &
579 Sons.
580 Egholm, D. L., Nielsen, S. B., Pedersen, V. K., & Lesemann, J. E. (2009). Glacial effects
581 limiting mountain height. *Nature*, 460, 884–887. Doi: 10.1038/nature08263
582 Egholm, D. L., Pedersen, V. K., Knudsen, M. F., & Larsen, N. K. (2012). Coupling the
583 flow of ice, water, and sediment in a glacial landscape evolution
584 model. *Geomorphology*, 141, 47–66. Doi: 10.1016/j.geomorph.2011.12.019
585 Evans, I.S. (2006). Allometric development of glacial cirque form: geological, relief and
586 regional effects on the cirques of Wales. *Geomorphology*, 80(3-4), 245–266. Doi:
587 10.1016/j.geomorph.2006.02.013
588 Evans, I. S., & Cox, N. J., 1974. Geomorphometry and the operational definition of
589 cirques. *Area*, 6, 150–153
590 Evans, I. S., & Cox, N. J. (1995). The form of glacial cirques in the English Lake District,
591 Cumbria. *Zeitschrift fur Geomorphologie, NF*, 39, 175–202.
592 Evans, I. S., & Cox, N. J. (2017). Comparability of cirque size and shape measures
593 between regions and between researchers. *Zeitschrift fur Geomorphologie,* 61,
594 Suppl. 2, 81–103. Doi: 10.1127/zfg_suppl/2016/0329
595 Fick, S. E., & Hijmans, R. J. (2017). WorldClim 2: new 1-km spatial resolution climate
596 surfaces for global land areas. *International Journal of Climatology*, 37(12), 4302–
597 4315. Doi: 10.1002/joc.5086

598 Gądek, B., Grabiec, M., & Kędzia, S. (2015). Application of Ground Penetrating Radar to
599 Identification of Thickness and Structure of Sediments in Postglacial Lakes,
600 Illustrated with an Example of the Mały Staw Lake (The Karkonosze
601 Mountains). *Studia Geomorphologica Carpatho-Balcanica*, 49(1), 5–13. Doi:
602 10.1515/sgcb-2015-0006
603 Gordon, J. E. (1977). Morphometry of cirques in the Kintail-Affric-Cannich area of
604 northwest Scotland. *Geografiska Annaler: Series A, Physical Geography*, 59(3-4),
605 177–194. Doi: 10.2307/520798
606 Graf, W. L. (1976). Cirques as glacier locations. *Arctic and Alpine Research*. 8, 79–90.
607 Doi: 10.2307/1550611
608 Hallet, B., Hunter, L., & Bogen, J. (1996). Rates of erosion and sediment evacuation by
609 glaciers: A review of field data and their implications. *Global and Planetary*
610 *Change*, *12*(1-4), 213–235. Doi: 10.1016/0921-8181(95)00021-6
611 Hannah, D. M., Gurnell, A. M., & Mcgregor, G. R. (2000). Spatio–temporal variation in
612 microclimate, the surface energy balance and ablation over a cirque
613 glacier. *International Journal of Climatology*, 20(7), 733–758. Doi: 10.1002/1097-
614 0088(20000615)20:7<733::AID-JOC490>3.0.CO;2-F
615 Harrison, S., Rowan, A. V., Glasser, N. F., Knight, J., Plummer, M. A., & Mills, S. C.
616 (2014). Little Ice Age glaciers in Britain: Glacier–climate modelling in the
617 Cairngorm mountains. *The Holocene*, 24(2), 135–140. Doi:
618 10.1177/0959683613516170
619 Hicks, D. M., McSaveney, M. J., & Chinn, T. J. H. (1990). Sedimentation in proglacial
620 Ivory Lake, Southern Alps, New Zealand. *Arctic and Alpine Research*, 22(1), 26–
621 42. Doi: 10.1080/00040851.1990.12002763

622 Hock, R. (2003). Temperature index melt modelling in mountain areas. *Journal of*
623 *hydrology*, 282(1-4), 104–115. Doi: 10.1016/S0022-1694(03)00257-9
624 Hooke, R. L., (1991). Positive feedbacks associated with erosion of glacial cirques and
625 overdeepenings. *Geological Society of America Bulletin*, *103*(8), 1104–1108. Doi:
626 10.1130/0016-7606(1991)103<1104:PFAWEO>2.3.CO;2
627 Koppes, M. N., & Montgomery, D. R. (2009). The relative efficacy of fluvial and glacial
628 erosion over modern to orogenic timescales. *Nature Geoscience*, 2(9), 644–647.
629 Doi: 10.1038/ngeo616
630 Larsen, E., & Mangerud, J. (1981). Erosion rate of a Younger Dryas cirque glacier at
631 Krakenes, western Norway. *Annals of Glaciology*, 2(1), 153–158. Doi:
632 10.3189/172756481794352216
633 Laumann, T., & Reeh, N. (1993). Sensitivity to climate change of the mass balance of
634 glaciers in southern Norway. *Journal of Glaciology*, 39, 656–665. Doi:
635 10.3189/S0022143000016555
636 Lewis, W. V. (1949). Glacial movement by rotational slipping. *Geografiska Annaler*, 31(1-
637 4), 146–158. Doi: 10.1080/20014422.1949.11880800
638 Lisiecki, L. E., & Raymo, M. E. (2005). A Pliocene-Pleistocene stack of 57 globally
639 distributed benthic $\delta^{18}O$ records. *Paleoceanography*, 20, PA1003. Doi:
640 10.1029/2004PA001071
641 MacGregor, K. R., Anderson, R. S., & Waddington, E. D. (2009). Numerical modeling of
642 glacial erosion and headwall processes in alpine valleys. *Geomorphology*, *103*(2),
643 189–204. Doi: 10.1016/j.geomorph.2008.04.022
644 Mathews, W. H. (1947). "Tuyas," flat-topped volcanoes in northern British
645 Columbia. *American Journal of Science*, 245(9), 560–570. Doi:
646 10.2475/ajs.245.9.560

647 Mills, H. H. (1979). Some implications of sediment studies for glacial erosion on Mount
648 Rainier, Washington. *Northwest Science*, 53(3), 190–199.
649 Mîndrescu, M., Evans, I. S., & Cox, N. J. (2010). Climatic implications of cirque
650 distribution in the Romanian Carpathians: palaeowind directions during glacial
651 periods. *Journal of Quaternary Science*, 25(6), 875–888. Doi: 10.1002/jqs.1363
652 Mitchell, S. G., & Humphries, E. E. (2015). Glacial cirques and the relationship between
653 equilibrium line altitudes and mountain range height. *Geology*, 43(1), 35–38. Doi:
654 10.1130/G36180.1
655 Olyphant, G. A. (1981). Allometry and cirque evolution. *Geological Society of America*
656 *Bulletin*, 92(9), 679–685. Doi: 10.1130/0016-7606(1981)92<679:AACE>2.0.CO;2
657 Oskin, M., & Burbank, D. W. (2005). Alpine landscape evolution dominated by cirque
658 retreat. *Geology*, *33*(12), 933–936. Doi: 10.1130/G21957.1
659 Pedersen, V. K., Huismans, R. S., Herman, F., & Egholm, D. L. (2014). Controls of initial
660 topography on temporal and spatial patterns of glacial
661 erosion. *Geomorphology*, *223*, 96–116. Doi: 10.1016/j.geomorph.2014.06.028
662 Pedersen, V. K., Egholm, D. L., & Nielsen, S. B. (2010). Alpine glacial topography and
663 the rate of rock column uplift: a global perspective. *Geomorphology*, 122(1-2),
664 129–139. Doi: 10.1016/j.geomorph.2010.06.005
665 Reheis, M. J. (1975). Source, transportation and deposition of debris on Arapaho glacier,
666 Front Range, Colorado, USA. *Journal of Glaciology*, 14(7), 407–420. Doi:
667 10.3189/S0022143000021936
668 Rolland, C. (2003). Spatial and seasonal variations of air temperature lapse rates in
669 Alpine regions. *Journal of Climate*, 16(7), 1032–1046. Doi: 10.1175/1520-
670 0442(2003)016<1032:SASVOA>2.0.CO;2

671 Sanders, J. W., Cuffey, K. M.,MacGregor, K. R., & Collins, B. D. (2013). The sediment
672 budget of an alpine cirque. *Geological Society of America Bulletin*, 125, 229–248.
673 Doi: 10.1130/B30688.1
674 Sanders, J. W., Cuffey, K. M., Moore, J. R., MacGregor, K. R., & Kavanaugh, J. L. (2012).
675 Periglacial weathering and headwall erosion in cirque glacier
676 bergschrunds. *Geology*, *40*(9), 779–782. Doi 10.1130/G33330.1
677 Seguinot, J., Ivy-Ochs, S., Jouvet, G., Huss, M., Funk, M., & Preusser, F. (2018).
678 Modelling last glacial cycle ice dynamics in the Alps. *The Cryosphere*, 12(10),
679 3265–3285. Doi: 10.5194/tc-12-3265-2018
680 Smellie, J. L. (2017). Glaciovolcanism: A 21st Century Proxy for Palaeo-Ice. In Menzies,
681 J., & van der Meer, J., (Eds.), *Past Glacial Environments* 2nd Edition (pp. 335–
682 375). Elsevier. Doi: 10.1016/B978-0-08-100524-8.00010-5
683 Smellie, J. L., & Edwards, B. R. (2016). *Glaciovolcanism on Earth and Mars*.
684 Cambridge: Cambridge University Press. Doi: 10.1017/CBO9781139764384
685 Spagnolo, M., Pellitero, R., Barr, I. D., Ely, J. C., Pellicer, X. M., & Rea, B.R. (2017).
686 ACME, a GIS tool for automated cirque metric extraction. *Geomorphology*, 278,
687 280–286. Doi: 10.1016/j.geomorph.2016.11.018
688 Turnbull, J. M. & Davies, R. H. (2006). A mass movement origin for cirques. *Earth*
689 *Surface Processes and Landforms*, 31, 1129–1148. Doi: 10.1002/esp.1324
690
691
692
693
694
695

Supplementary material 1.

Model validation and sensitivity

1. Comparison with glacier-climate modelling

Though we model ice accumulation for all cirques in Britain and Ireland (Section 2.2.), in order to validate this approach we make a direct comparison with Harrison et al. (2014), who use glacier-climate modelling to reconstruct Little Ice Age (LIA) cirque glaciers in the northern Cairngorms. Harrison et al. (2014) use a two-dimensional glaciological model (based on Plummer & Phillips, 2003), which is more complex than the model used in the present study (i.e., we only model the spatial extent of the zone of former ice accumulation, not glacier dimensions). For example, Harrison et al. (2014) not only consider atmospheric and topographic controls on surface energy balance, but also account for the role of avalanching of snow from adjacent slopes. Since Harrison et al. (2014) focus on a comparatively small region (~10 km x 6 km), their modelling approach also differs from ours in that monthly mean meteorological data are derived directly from two local automatic weather stations, rather than from gridded sources. They also define their model domain using the ASTER GDEM v.2 digital elevation model, rather than the SRTM data we use. Despite these differences, the modelling of Harrison et al. (2014) provides a useful means of validating our approach.

For comparison, we first forced our model with contemporary climate (i.e., $\Delta T = 0°C$, $P = 100\%$). This resulted in small areas of ice accumulation in the high-elevation cirques (Supplementary Fig. 1a), similar to those modelled by Harrison et al. (2014) (Supplementary Fig. 1c). To simulate LIA conditions (as defined by Harrison et al., 2014), the model was then run with ΔT of -1.5 °C, and an increase in precipitation of

721 10%, relative to present (i.e., ΔT = -1.5°C, P = 110%). This revealed a total ice
722 accumulation area of 2.65 km^2 (Supplementary Fig. 1b), and a full glacial area
723 (assuming an accumulation area ratio of 0.5) of ~5.3 km^2, which compares with the
724 total glaciated area of 7.54 km^2 modelled by Harrison et al (2014) (Supplementary Fig.
725 1d).

726 In our model (as in Harrison et al., 2014), ice accumulation shows sensitivity
727 to both temperature and precipitation. For example, when ΔT was shifted from -1.5°C
728 to -2°C, the area of ice accumulation in the northern Cairngorms study site (shown in
729 Supplementary Fig. 1) increased from 2.65 to 3.57 km^2, and an increase in
730 precipitation from +10% to +20% (ΔT = -1.5°C), relative to present, increased the area
731 of ice accumulation by 0.17 km^2. Under LIA conditions (i.e., ΔT = -1.5°C, P = 110%),
732 changing *DDF* from a value that ranged on a pixel-by-pixel basis (as outlined in Section
733 2.2.), to a constant value of 4.1 reduced the area of ice accumulation by 0.86 km^2.
734 Limiting ice accumulation to slopes <60°, rather than <30° increased the area of ice
735 accumulation by 0.77 km^2. Finally, lowering T_{crit} from 2°C to 0°C reduced the area of
736 ice accumulation by 0.74 km^2.

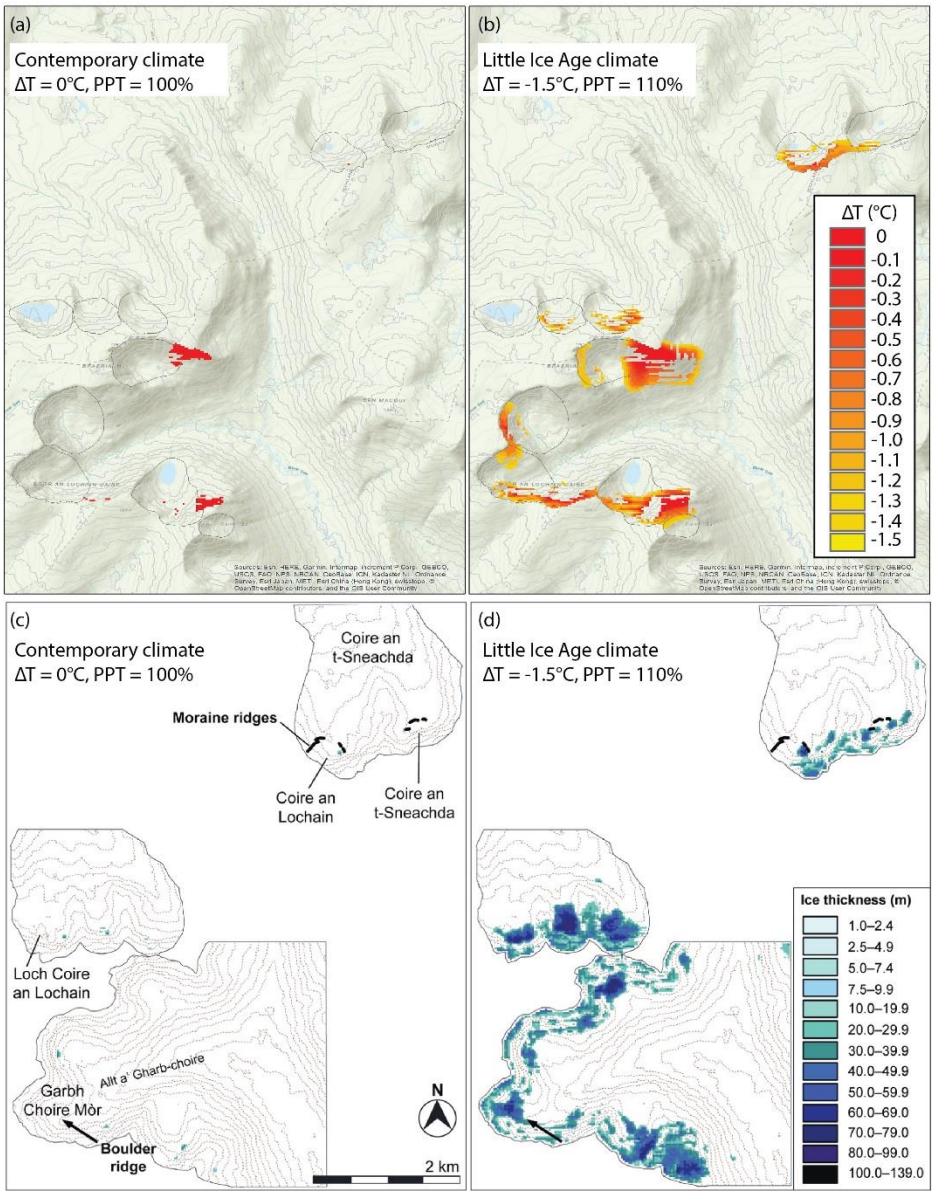

737

738 Supplementary Fig. 1. The zone of ice accumulation, as modelled in the present study,
739 in the northern Cairngorms, under (a) contemporary (ΔT = 0°C and P = 100%), and
740 (b) Little Ice Age conditions (ΔT = −1.5°C and P = 110%). In (a) and (b) colours
741 represent the temperature depression (relative to present) required for ice to
742 accumulate. (c) and (d) show glaciers, as simulated by Harrison et al. (2014), in this
743 same region, under contemporary and Little Ice Age conditions, respectively. In (c)
744 and (d), colours represent ice thickness.

745

2. Comparison with published equilibrium-line altitude estimates

As a second approach to validate the ice accumulation modelling, we make a comparison with geomorphologically constrained reconstructions of former glaciers in Britain and Ireland. Specifically, we compare past glacier equilibrium-line altitudes (ELAs), as derived from published ice mass reconstructions, with ELAs derived through our ice accumulation modelling (i.e., within each cirque, under given climate, we assume that the altitude of the lowest pixel accumulating ice reflects the ELA). We focus exclusively on reconstructions of small glaciers, since our model domain is constrained to cirques (the focus of our investigation). In total, we make a comparison with ELA estimates from 88 reconstructed cirque glaciers (Supplementary Table. 1).

Results indicate a clear correspondence between geomorphologically derived (published) and modelled (from the present study) ELA estimates (Supplementary Fig. 2). The average elevation difference between these ELA estimates is 75 m, and, in all but three cases, the elevation difference for individual glaciers is <150 m. The three exceptions to this are sites in Ireland (Carrawaystick, Logaharry, and Sruhauncullinmore), where Barth et al. (2017) reconstruct glaciers at periods (i.e., 10.8 ± 0.5 ka, 14.2 ± 0.3 ka, and 11.1 ± 0.4 ka) when GRIP data suggest comparatively high temperatures (and therefore high ELAs—Supplementary Fig. 2). These differences in ELA estimates partly reflect difficulties with using GRIP climate data to model specific glaciers in distal sites such as Britain and Ireland, but are also strongly controlled by the precise time period suggested by geochronometric dating. For example, if the time intervals suggested by Barth et al. (2017) are altered by ± 0.5 ka, then elevation differences between modelled and published ELA estimates for all glaciers are <150 m. In all, this comparison demonstrates that there are some differences between geomorphologically derived (published) and modelled (from the

present study) ELA estimates, but that given the broad scale approach used to model ice accumulation, and the use of distal palaeoclimate data (i.e., GRIP), such discrepancies are expected (at least for some individual glaciers). It is also reassuring to note that in most cases, published and modelled ELA estimates are closely related (Supplementary Fig. 2).

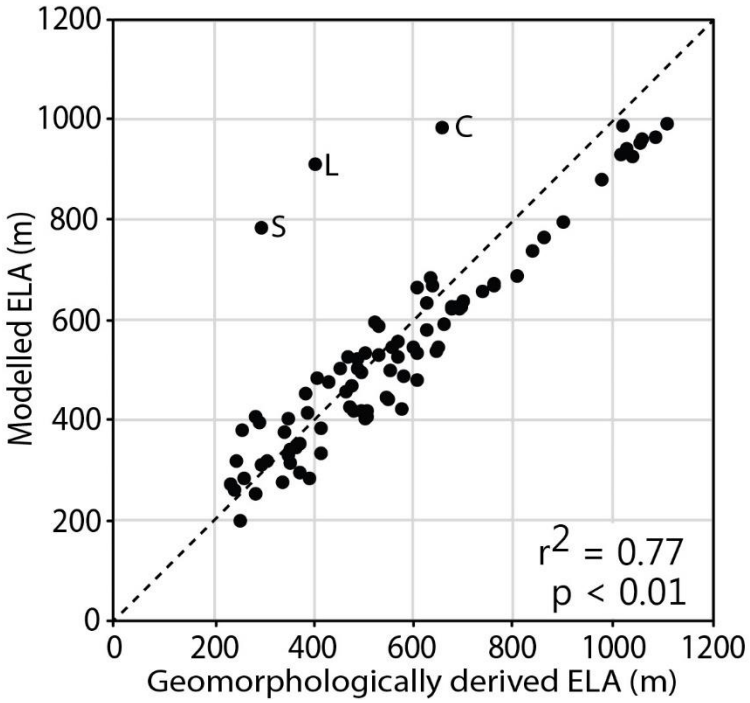

Supplementary Fig. 2. Comparison between geomorphologically derived (published) and modelled (from the present study) equilibrium-line altitude (ELA) estimates for 88 former cirque glaciers in Britain and Ireland (Supplementary Table 1). Labelled points are palaeoglaciers mentioned in the text: C= Carrawaystick, L =Logaharry, and S = Sruhauncullinmore. Details are provided in Supplementary Table. 1.

Supplementary Table. 1. Comparison between geomorphologically derived (published) and modelled (from the present study) equilibrium-line altitude (ELA) estimates for 88 former cirque glaciers in Britain and Ireland.

Palaeoglaicer name	Lat (DD)	Lon (DD)	Time period (ka)	Published ELA (m)	Our ELA (m)	Citation
Alohart	52.01	-9.67	20.5 ± 0.6	370	299	Barth et al (2017)
An Clù-nead.	58.00	-5.23	12.9–11.7	305	322	Chandler & Lukas (2017)
Arkle corrie (North)	58.37	-4.89	12.9–11.7	412	387	Lukas & Bradwell (2010)
Arkle corrie (South)	58.36	-4.87	12.9–11.7	370	358	Lukas & Bradwell (2010)
Blindtarn Moss	54.46	-3.06	12.9–11.7	292	316	Wilson (2002)
Bunnafreva	53.99	-10.18	20.5 ± 0.4	350	318	Barth et al (2017)
Bunnafreva	53.99	-10.18	18.8 ± 0.4	360	349	Barth et al (2017)
Cadh' a' Mhoraire	57.99	-5.20	12.9–11.7	345	334	Chandler & Lukas (2017)
Carrawaystick	52.96	-6.43	10.8 ± 0.5	655	988	Barth et al (2017)
Cleister glacier	57.97	-6.93	12.9–11.7	251	205	Ballantyne (2007b)
Coire a'Bhradain Glacier	55.61	-5.23	12.9–11.7	494	423	Ballantyne (2007a)
Coire an Lochain (Braeriach)	57.10	-3.68	12.9–11.7	1037	932	Standell (2014)
Coire an Lochain (Cairn Gorm)	57.08	-3.74	12.9–11.7	1019	991	Standell (2014)
Coire an t-Saighdeir (Glen Dee)	57.05	-3.71	12.9–11.7	1058	964	Standell (2014)
Coire an t-Sneachda	57.11	-3.66	12.9–11.7	1026	945	Standell (2014)
Coire Bhrochain (Braeriach)	57.08	-3.72	12.9–11.7	1082	968	Standell (2014)
Coire Bogha-cloiche	57.08	-3.76	12.9–11.7	977	885	Standell (2014)
Coire Clachach	56.47	-5.79	12.9–11.7	252	383	Ballantyne (2002)
Coire Dhondail	57.06	-3.78	12.9–11.7	899	800	Standell (2014)
Coire Dubh glacier	57.96	-6.83	12.9–11.7	289	401	Ballantyne (2007b)
Coire Garbhlach	57.03	-3.84	12.9–11.7	804	692	Standell (2014)

Coire Gorm	56.42	-6.02	12.9–11.7	551	504	Ballantyne (2002)
Coire Lan Glacier	55.63	-5.19	12.9–11.7	631	687	Ballantyne (2007a)
Coire na Beinn Fada	56.43	-6.01	12.9–11.7	485	528	Ballantyne (2002)
Coire na Ciche (Beinn a' Bhuird)	57.07	-3.49	12.9–11.7	1014	935	Standell (2014)
Coire na Saobhaidh (Glen Derry)	57.04	-3.60	12.9–11.7	760	677	Standell (2014)
Coire nan Ceum Glacier	55.66	-5.22	12.9–11.7	504	421	Ballantyne (2007a)
Coire nan Gabhar	56.45	-6.00	12.9–11.7	410	338	Ballantyne (2002)
Coire nan Larach Glacier	55.64	-5.18	12.9–11.7	572	428	Ballantyne (2007a)
Coire Ruadh	57.08	-3.73	12.9–11.7	1106	996	Standell (2014)
Corranabinna	53.97	-9.68	19.4 ± 0.5	350	345	Barth et al (2017)
Corranabinna	53.97	-9.68	15.4 ± 0.6	470	429	Barth et al (2017)
Craig Cerrig-gleisiad	51.89	-3.51	12.9–11.7	486	509	Carr et al (2010)
Cwm Anafon glacier	53.20	-3.95	12.9–11.7	603	670	Bendle & Glasser (2012)
Cwm Bleiddiaid glacier	53.01	-4.14	12.9–11.7	502	409	Bendle & Glasser (2012)
Cwm Bochlywyd glacier	53.11	-4.01	12.9–11.7	674	627	Bendle & Glasser (2012)
Cwm Bual glacier	53.13	-4.05	12.9–11.7	603	483	Bendle & Glasser (2012)
Cwm Bychan glacier	53.14	-3.94	12.9–11.7	637	671	Bendle & Glasser (2012)
Cwm Caseg glacier	53.17	-3.98	12.9–11.7	837	741	Bendle & Glasser (2012)
Cwm Clogwyn glacier	53.08	-4.10	12.9–11.7	520	598	Bendle & Glasser (2012)
Cwm Clyd glacier	53.12	-4.04	12.9–11.7	760	673	Bendle & Glasser (2012)
Cwm Coch glacier	53.13	-4.05	12.9–11.7	463	463	Bendle & Glasser (2012)
Cwm Cywion glacier	53.12	-4.05	12.9–11.7	675	630	Bendle & Glasser (2012)
Cwm Drws-y-Coed glacier	53.05	-4.17	12.9–11.7	380	458	Bendle & Glasser (2012)
Cwm Du'r Arddu glacier	53.08	-4.09	12.9–11.7	624	583	Bendle & Glasser (2012)

Cwm Dulyn glacier	53.18	-3.95	12.9–11.7	642	544	Bendle & Glasser (2012)
Cwm Dwythwch (i) glacier	53.09	-4.15	12.9–11.7	467	532	Bendle & Glasser (2012)
Cwm Dwythwch (ii) glacier	53.09	-4.14	12.9–11.7	475	472	Bendle & Glasser (2012)
Cwm Eigiau (i) glacier	53.15	-3.93	12.9–11.7	502	537	Bendle & Glasser (2012)
Cwm Eigiau (ii) glacier	53.15	-3.95	12.9–11.7	605	539	Bendle & Glasser (2012)
Cwm Ffynnon-y-Gwas glacier	53.08	-4.10	12.9–11.7	452	506	Bendle & Glasser (2012)
Cwm Glas Mawr glacier	53.08	-4.06	12.9–11.7	383	419	Bendle & Glasser (2012)
Cwm Graianog glacier	53.14	-4.06	12.9–11.7	545	444	Bendle & Glasser (2012)
Cwm Idwal glacier	53.11	-4.03	12.9–11.7	505	413	Bendle & Glasser (2012)
Cwm Lloer glacier	53.14	-4.01	12.9–11.7	737	660	Bendle & Glasser (2012)
Cwm Llugwy glacier	53.15	-3.96	12.9–11.7	660	596	Bendle & Glasser (2012)
Cwm Siabod glacier	53.08	-3.92	12.9–11.7	596	548	Bendle & Glasser (2012)
Cwm Silyn glacier	53.03	-4.22	12.9–11.7	427	480	Bendle & Glasser (2012)
Cwm Tregalan glacier	53.06	-4.07	12.9–11.7	648	551	Bendle & Glasser (2012)
Cwm Tryfan glacier	53.11	-3.99	12.9–11.7	579	492	Bendle & Glasser (2012)
Cwm year Hafod glacier	53.10	-4.15	12.9–11.7	527	533	Bendle & Glasser (2012)
Cwmglas Bach glacier	53.15	-4.01	12.9–11.7	684	632	Bendle & Glasser (2012)
Cwmglas Mawr glacier	53.15	-3.99	12.9–11.7	689	625	Bendle & Glasser (2012)
Cwmorthin glacier	53.00	-3.98	12.9–11.7	402	488	Bendle & Glasser (2012)
Cwm-y-Ffynnon glacier	53.04	-4.18	12.9–11.7	476	424	Bendle & Glasser (2012)
Cwm-y-Gors glacier	53.11	-3.96	12.9–11.7	387	290	Bendle & Glasser (2012)
Ealta Choire Glacier	55.62	-5.24	12.9–11.7	567	531	Ballantyne (2007a)
Fan Fawr	51.86	-3.49	12.9–11.7	623	640	Carr et al (2010)
Garbh Choire Glacier	55.66	-5.24	12.9–11.7	543	448	Ballantyne (2007a)

Glascairns Hill	54.77	-8.03	15.9 ± 0.5	340	380	Barth et al (2017)
Glascairns Hill	54.77	-8.03	12.0 ± 0.6	345	407	Barth et al (2017)
Gleann Bearraray glacier	58.01	-6.97	12.9–11.7	237	264	Ballantyne (2007b)
Glen Scaladale glacier	57.97	-6.82	12.9–11.7	257	288	Ballantyne (2007b)
Glen Skeaudale glacier	57.93	-6.80	12.9–11.7	229	277	Ballantyne (2007b)
Llydaw glacier	53.07	-4.06	12.9–11.7	567	560	Bendle & Glasser (2012)
Lochan nan Gabhar	57.11	-3.41	12.9–11.7	860	768	Standell (2014)
Lochan Uaine (Ben Macdui)	57.06	-3.65	12.9–11.7	1052	956	Standell (2014)
Logaharry	53.62	-9.70	14.2 ± 0.3	400	917	Barth et al (2017)
Lough Accorymore	53.99	-10.18	18.4 ± 0.5	240	322	Barth et al (2017)
Lough Accorymore	53.99	-10.18	17.2 ± 0.3	280	412	Barth et al (2017)
Marchlyn Bach glacier	53.14	-4.08	12.9–11.7	554	550	Bendle & Glasser (2012)
Marchlyn Mawr glacier	53.14	-4.07	12.9–11.7	692	632	Bendle & Glasser (2012)
Melynllyn glacier	53.17	-3.94	12.9–11.7	696	641	Bendle & Glasser (2012)
Moelwyn Mawr glacier	52.99	-4.00	12.9–11.7	526	592	Bendle & Glasser (2012)
Nine Gills Comb	54.68	-3.12	12.9–11.7	492	501	Wilson & Clark (1999)
Sgùrr an Fhidleir	58.00	-5.22	12.9–11.7	335	279	Chandler & Lukas (2017)
Sruhauncullinmore	53.65	-9.80	12.3 ± 0.4	280	256	Barth et al (2017)
Sruhauncullinmore	53.65	-9.80	11.1 ± 0.4	290	788	Barth et al (2017)

787

788

789

790

791 **Additional references for Supplementary material**

792 Ballantyne, C. K. (2002). The Loch Lomond Readvance on the Isle of Mull, Scotland:
793 glacier reconstruction and palaeoclimatic implications. *Journal of Quaternary*
794 *Science: Published for the Quaternary Research Association*, *17*(8), 759–771.
795 Doi: 10.1002/jqs.729
796 Ballantyne, C. K. (2007a). The Loch Lomond Readvance on north Arran, Scotland:
797 glacier reconstruction and palaeoclimatic implications. *Journal of Quaternary*
798 *Science: Published for the Quaternary Research Association*, *22*(4), 343–359.
799 Doi: 10.1002/jqs.1059
800 Ballantyne, C. K. (2007b). Loch Lomond Stadial glaciers in North Harris, Outer
801 Hebrides, North-West Scotland: glacier reconstruction and palaeoclimatic
802 implications. *Quaternary Science Reviews*, *26*(25-28), 3134–3149. Doi:
803 10.1016/j.quascirev.2007.09.001
804 Barth, A. M., Clark, P. U., Clark, J., Roe, G. H., Marcott, S. A., McCabe, A. M., Caffee,
805 M. W., He, F., Cuzzone, J. K., & Dunlop, P. (2017). Persistent millennial-scale
806 glacier fluctuations in Ireland between 24 ka and 10 ka. *Geology*, *46*(2), 151–154.
807 Doi: 10.1130/G39796.1
808 Bendle, J. M., & Glasser, N. F. (2012). Palaeoclimatic reconstruction from lateglacial
809 (younger dryas chronozone) cirque glaciers in snowdonia, north
810 wales. *Proceedings of the Geologists' Association*, *123*(1), 130–145. Doi:
811 10.1016/j.pgeola.2011.09.006
812 Carr, S. J., Lukas, S., & Mills, S. C. (2010). Glacier reconstruction and mass-balance
813 modelling as a geomorphic and palaeoclimatic tool. *Earth Surface Processes and*
814 *Landforms*, *35*(9), 1103–1115. Doi: 10.1002/esp.2034
815 Chandler, B. M., & Lukas, S. (2017). Reconstruction of Loch Lomond Stadial (Younger
816 Dryas) glaciers on Ben More Coigach, north-west Scotland, and implications for

reconstructing palaeoclimate using small ice masses. *Journal of Quaternary Science*, *32*(4), 475–492. Doi: 10.1002/jqs.2941

Lukas, S., & Bradwell, T. (2010). Reconstruction of a Lateglacial (Younger Dryas) mountain ice field in Sutherland, northwestern Scotland, and its palaeoclimatic implications. *Journal of Quaternary Science: Published for the Quaternary Research Association*, *25*(4), 567–580. Doi: 10.1002/jqs.1376

Plummer, M. A., & Phillips, F. M. (2003). A 2-D numerical model of snow/ice energy balance and ice flow for paleoclimatic interpretation of glacial geomorphic features. *Quaternary Science Reviews*, 22(14), 1389–1406. Doi: 10.1016/S0277-3791(03)00081-7

Standell, M. R. (2014). Lateglacial (Younger Dryas) glaciers and ice-sheet deglaciation in the Cairngorm Mountains, Scotland: glacier reconstructions and their palaeoclimatic implications (Doctoral dissertation). Retrieved from Loughborough University Institutional Repository (https://dspace.lboro.ac.uk/2134/16159).

Wilson, P. (2002). Morphology and significance of some Loch Lomond Stadial moraines in the south-central Lake District, England. *Proceedings of the Geologists' Association*, *113*(1), 9–21. Doi: 10.1016/S0016-7878(02)80002-5

Wilson, P., & Clark, R. (1999). Further glacier and snowbed sites of inferred Loch Lomond Stadial age in the northern Lake District, England. *Proceedings of the Geologists' Association*, *110*(4), 321–331. Doi: 10.1016/S0016-7878(99)80026-1